Indication for the disappearance of reactor $\bar{\nu}_e$ in the Double Chooz experiment

Y. Abe,[28] C. Aberle,[21] T. Akiri,[4,15] J.C. dos Anjos,[5] F. Ardellier,[15] A.F. Barbosa,[5] A. Baxter,[26] A. Bernstein,[16] T.J.C. Bezerra,[30] L. Bezrukhov,[14] E. Blucher,[6] M. Bongrand,[15,30] N.S. Bowden,[16] C. Buck,[21] J. Busenitz,[2] A. Cabrera,[4] E. Caden,[10] L. Camilleri,[8] R. Carr,[8] M. Cerrada,[7] P.-J. Chang,[17] P. Chimenti,[34] T. Classen,[9,16] A. Collin,[15] E. Conover,[6] J.M. Conrad,[20] S. Cormon,[25] J.I. Crespo-Anadón,[7] M. Cribier,[15,4] K. Crum,[6] A. Cucoanes,[25,15] M.V. D'Agostino,[3] E. Damon,[10] J.V. Dawson,[4] S. Dazeley,[16] M. Dierckxsens,[6] D. Dietrich,[33] Z. Djurcic,[3] M. Dracos,[24] V. Durand,[15,4] Y. Efremenko,[27] Y. Endo,[29] A. Etenko,[19] E. Falk,[26] M. Fallot,[25] M. Fechner,[15] F. von Feilitzsch,[31] J. Felde,[9] S.M. Fernandes,[26] D. Franco,[4] A. Franke,[8] M. Franke,[31] H. Furuta,[30] R. Gama,[5] I. Gil-Botella,[7] L. Giot,[25] M. Göger-Neff,[31] L.F.G. Gonzalez,[35] M.C. Goodman,[3] J.TM. Goon,[2] D. Greiner,[33] B. Guillon,[25] N. Haag,[31] C. Hagner,[11] T. Hara,[18] F.X. Hartmann,[21] J. Hartnell,[26] T. Haruna,[29] J. Haser,[21] A. Hatzikoutelis,[27] T. Hayakawa,[22,15] M. Hofmann,[31] G. Horton-Smith,[17] M. Ishitsuka,[28] J. Jochum,[33] C. Jollet,[24] C.L. Jones,[20] F. Kaether,[21] L. Kalousis,[24] Y. Kamyshkov,[27] D. Kaplan,[13] T. Kawasaki,[22] G. Keefer,[16] E. Kemp,[35] H. de Kerret,[4] Y. Kibe,[28] T. Konno,[28] D. Kryn,[4] M. Kuze,[28] T. Lachenmaier,[33] C.E. Lane,[10] C. Langbrandtner,[21] T. Lasserre,[15,4] A. Letourneau,[15] D. Lhuillier,[15] H.P. Lima Jr,[5] M. Lindner,[21] Y. Liu,[2] J.M. López-Castanõ,[7] J.M. LoSecco,[23] B.K. Lubsandorzhiev,[14] S. Lucht,[1] D. McKee,[2,17] J. Maeda,[29] C.N. Maesano,[9] C. Mariani,[8] J. Maricic,[10] J. Martino,[25] T. Matsubara,[29] G. Mention,[15] A. Meregaglia,[24] T. Miletic,[10] R. Milincic,[10] A. Milzstajn,[15,*] H. Miyata,[22] D. Motta,[15,*] Th.A. Mueller,[15,30] Y. Nagasaka,[12] K. Nakajima,[22] P. Novella,[7] M. Obolensky,[4] L. Oberauer,[31] A. Onillon,[25] A. Osborn,[27] I. Ostrovskiy,[2] C. Palomares,[7] S.J.M. Peeters,[26] I.M. Pepe,[5] P. Perrin,[15] P. Pfahler,[31] A. Porta,[25] W. Potzel,[31] R. Queval,[15] J. Reichenbacher,[2] B. Reinhold,[21] A. Remoto,[25,4] D. Reyna,[3] M. Röhling,[33] S. Roth,[1] H.A. Rubin,[13] Y. Sakamoto,[32] R. Santorelli,[7] F. Sato,[29] S. Schönert,[31] S. Schoppmann,[1] U. Schwan,[21] T. Schwetz,[21] M. Shaevitz,[8] D. Shrestha,[17] J-L. Sida,[15] V. Sinev,[14,15] M. Skorokhvatov,[19] E. Smith,[10] A. Stahl,[1] I. Stancu,[2] M. Strait,[6] A. Stüken,[1] F. Suekane,[30] S. Sukhotin,[19] T. Sumiyoshi,[29] Y. Sun,[2] Z. Sun,[15] R. Svoboda,[9] H. Tabata,[30] N. Tamura,[22] K. Terao,[20] A. Tonazzo,[4] M. Toups,[8] H.H. Trinh Thi,[31] C. Veyssiere,[15] D. Vignaud,[4] S. Wagner,[21] H. Watanabe,[21] B. White,[27] C. Wiebusch,[1] L. Winslow,[20] M. Worcester,[6] M. Wurm,[11] E. Yanovitch,[14] F. Yermia,[25] K. Zbiri,[25,10] and V. Zimmer[31]

(Double Chooz Collaboration)

[1] *RWTH Aachen University, 52056 Aachen, Germany*
[2] *Department of Physics and Astronomy, University of Alabama, Tuscaloosa, Alabama 35487, USA*
[3] *Argonne National Laboratory, Argonne, Illinois 60439, USA*
[4] *APC, AstroParticule et Cosmologie, Université Paris Diderot, CNRS/IN2P3, CEA/IRFU, Observatoire de Paris, Sorbonne Paris Citë, 75205 Paris Cedex 13, France*
[5] *Centro Brasileiro de Pesquisas Físicas, Rio de Janeiro, RJ, cep 22290-180, Brazil*
[6] *The Enrico Fermi Institute, The University of Chicago, Chicago, IL 60637, USA*
[7] *Centro de Investigaciones Energéticas, Medioambientales y Tecnológicas, CIEMAT, E-28040, Madrid, Spain*
[8] *Columbia University; New York, NY 10027, USA*
[9] *University of California, Davis, CA-95616-8677, USA*
[10] *Physics Department, Drexel University, Philadelphia, Pennsylvania 19104, USA*
[11] *Institut für Experimentalphysik, Universität Hamburg, 22761 Hamburg, Germany*
[12] *Hiroshima Institute of Technology, Hiroshima, 731-5193, Japan*
[13] *Department of Physics, Illinois Institute of Technology, Chicago, Illinois 60616, USA*
[14] *Institute of Nuclear Research of the Russian Aacademy of Science, Russia*
[15] *Commissariat à l'Energie Atomique et aux Energies Alternatives, Centre de Saclay, IRFU, 91191 Gif-sur-Yvette, France*
[16] *Lawrence Livermore National Laboratory, Livermore, CA 94550, USA*
[17] *Department of Physics, Kansas State University, Manhattan, Kansas 66506, USA*
[18] *Department of Physics, Kobe University, Kobe, 657-8501, Japan*
[19] *NRC Kurchatov Institute, 123182 Moscow, Russia*
[20] *Massachusetts Institute of Technology; Cambridge, MA 02139, USA*
[21] *Max-Planck-Institut für Kernphysik, 69029 Heidelberg, Germany*
[22] *Department of Physics, Niigata University, Niigata, 950-2181, Japan*
[23] *University of Notre Dame, Notre Dame, IN 46556-5670, USA*
[24] *IPHC, Université de Strasbourg, CNRS/IN2P3, F-67037 Strasbourg, France*
[25] *SUBATECH, CNRS/IN2P3, Université de Nantes, Ecole des Mines de Nantes, F-44307 Nantes, France*
[26] *Department of Physics and Astronomy, University of Sussex, Falmer, Brighton BN1 9QH, United Kingdom*
[27] *Department of Physics and Astronomy, University of Tennessee, Knoxville, Tennessee 37996, USA*
[28] *Department of Physics, Tokyo Institute of Technology, Tokyo, 152-8551, Japan*
[29] *Department of Physics, Tokyo Metropolitan University, Tokyo, 192-0397, Japan*

[30] *Research Center for Neutrino Science, Tohoku University, Sendai 980-8578, Japan*
[31] *Physik Department, Technische Universität München, 85747 Garching, Germany*
[32] *Tohoku Gakuin University, Sendai, 981-3193, Japan*
[33] *Kepler Center for Astro and Particle Physics, Universität Tübingen, 72076, Tübingen, Germany*
[34] *Universidade Federal do ABC, UFABC, Sao Paulo, Santo André, SP, Brazil*
[35] *Universidade Estadual de Campinas-UNICAMP, Campinas, SP, Brazil*

(Dated: December 30, 2011)

The Double Chooz Experiment presents an indication of reactor electron antineutrino disappearance consistent with neutrino oscillations. A ratio of 0.944 ± 0.016 (stat) ± 0.040 (syst) observed to predicted events was obtained in 101 days of running at the Chooz Nuclear Power Plant in France, with two 4.25 GW_{th} reactors. The results were obtained from a single 10 m^3 fiducial volume detector located 1050 m from the two reactor cores. The reactor antineutrino flux prediction used the Bugey4 measurement as an anchor point. The deficit can be interpreted as an indication of a non-zero value of the still unmeasured neutrino mixing parameter $\sin^2 2\theta_{13}$. Analyzing both the rate of the prompt positrons and their energy spectrum we find $\sin^2 2\theta_{13} = 0.086 \pm 0.041$ (stat) ± 0.030 (syst), or, at 90% CL, $0.015 < \sin^2 2\theta_{13} < 0.16$.

PACS numbers: 14.60.Pq,13.15.+g,25.30.Pt,95.55.Vj,28.41.Ak
Keywords: neutrino oscillations, neutrino mixing, reactor

We report first results of a search for evidence of a non-zero neutrino oscillation[1] mixing angle, θ_{13}, based on the disappearance of reactor antineutrinos. This is the only one of the three mixing angles in the Pontecorvo-Maki-Nakagawa-Sakata matrix[2, 3] for which only upper limits[4][5] are available. The size of θ_{13} sets the required sensitivity of long-baseline oscillation experiments attempting to measure CP violation in the neutrino sector or the mass hierarchy. At accelerators using $\nu_\mu \to \nu_e$ appearance, the θ_{13} precision is affected by the added uncertainties associated with the CP violation parameter, δ, the sign of Δm^2_{atm}, and θ_{23}.

In reactor experiments[6, 7] addressing the disappearance of $\bar{\nu}_e$ the mixing angle θ_{13} determines the survival probability of electron antineutrinos at the "atmospheric" squared-mass difference, Δm^2_{atm}. This probability is given by:

$$P_{surv} \approx 1 - \sin^2 2\theta_{13} \sin^2(1.267 \Delta m^2_{atm} L/E) \,, \qquad (1)$$

where L is the distance from reactor to detector in meters and E the energy of the antineutrino in MeV. The full formula can be found in Ref. [1]. Eq. 1 provides a direct way to measure θ_{13} since the only additional input is the well measured value of $|\Delta m^2_{atm}| = (2.32^{+0.12}_{-0.08}) \times 10^{-3}$ eV^2 [8]. Indeed, other currently running reactor experiments [9], [10] are using the same technique.

Electron antineutrinos (< 9 MeV) produced by reactors are detected through inverse beta decay (IBD): $\bar{\nu}_e + p \to e^+ + n$. Detectors based on hydrocarbon liquid scintillators provide the free proton targets. The cross section, described in [11] and references therein, has a threshold of 1.81 MeV. The IBD signature is a coincidence of a prompt positron signal followed by a delayed neutron capture. The $\bar{\nu}_e$ energy, $E_{\bar{\nu}_e}$, is fully reconstructable from E_{prompt}, the positron visible energy ($E_{\bar{\nu}_e} \cong E_{prompt} + 0.78$ MeV).

Recently, indications of non-zero θ_{13} have been reported by two accelerator appearance experiments, T2K [12] and MINOS [13]. Various global fits (see e.g.[14, 15]) indicate central values in the range $0.05 < \sin^2 2\theta_{13} < 0.10$, accessible to the Double Chooz experiment[16][17].

We present here our first results with a single detector located ∼ 1050 m from the two 4.25 GW_{th} thermal power reactors of the Chooz Nuclear Power Plant and under a 300 MWE rock overburden. The analysis is based on data amounting to 101 effective days, mostly with both reactors on, but with 16 days with one reactor off and one day with both reactors off. The reactor flux estimate uses the Bugey4[18] results as an anchor point and is described below.

The emitted antineutrino flux mainly arises from the fissions of four isotopes (^{235}U, ^{239}Pu, ^{238}U, ^{241}Pu). The flux of each reactor depends on its thermal power and, for the four isotopes, their fractions of the total fuel content, their energy released per fission, and their fission and capture cross-sections.

The final error associated to the thermal power is ± 0.46% at full power [19, 20], fully correlated between the two cores. The fission rates and associated errors were evaluated using two commonly used predictive and complementary reactor simulation codes: MCNP Utility for Reactor Evolution (MURE)[21, 22] and DRAGON[23]. By computing the fission rates with these codes, a study of the sensitivity to the important reactor parameters (thermal power, boron concentration, temperatures and densities) was performed. The quality of these simulations was evaluated through benchmarks, such as the Takahama benchmark [24], and comparisons with Electricité de France (EDF) assembly simulations. The maximum discrepancies observed were included in the fission rate systematic error.

The MURE code was used to develop a 3D simulation of the two reactor cores. EDF provided the information required to simulate the fission rates including initial bur-

* Deceased.

nups of assemblies. To determine the inventories of each assembly composing the core at the startup of the data-taking cycle, assembly simulations were performed and the inventories at the given burnup were computed. The energies per fission computed by Kopeikin [25] and nuclear data evaluated from the JEFF3.1 database [26] were used. The evolution of the core simulations with time were then performed using as inputs the thermal power and the boron concentration from the EDF database averaged over 48 h time steps.

Relative contributions of the four main isotopes were deduced using the MURE simulation. The associated antineutrino flux was computed using the recently improved spectra from [27], converted from the ILL reference electron spectra [28–30], and the updated *ab initio* calculation of the ^{238}U spectrum[31]. The ILL spectra were measured after irradiating U or Pu for $\sim$ 1 day. Contributions from β-decays with lifetimes longer than these irradiation times were accounted for as prescribed in [31].

The Double Chooz detector system (Figure 1) consists of a main detector, an outer veto, and calibration devices. The main detector comprises four concentric cylindrical tanks filled with liquid scintillators or mineral oil.

The innermost 8 mm thick transparent (UV to visible) acrylic vessel houses the 10 m^3 ν-target liquid: a mixture of n-dodecane, PXE, PPO, bis-MSB and 1 g gadolinium/l as a beta-diketonate complex. The design emphasizes radiopurity and long term stability[32]. The ν-target volume is surrounded by the γ-catcher, a 55 cm thick Gd-free liquid scintillator layer in a second 12 mm thick acrylic vessel, used to detect γ-rays escaping from the ν-target. The light yield of the γ-catcher scintillator was matched to that of the ν-target scintillator to provide identical photoelectron (pe) yield across the full volume [33]. Outside the γ-catcher is the buffer, a 105 cm thick layer filled with mineral oil. It provides shielding from radioactivity of photomultipliers (PMTs) and of the surrounding rock, and is one of the major improvements over the CHOOZ experiment [4]. 390 10-inch PMTs [34–36] are installed on the stainless steel buffer tank inner wall to collect light from the inner volumes. These three volumes and the PMTs constitute the inner detector (ID). Outside the ID, and optically separated from it, is a 50 cm thick "inner veto" liquid scintillator (IV). The IV is equipped with 78 8-inch PMTs and functions as a cosmic muon veto and as a shield to spallation neutrons produced outside the detector. The whole detector is further surrounded by 15 cm of demagnetized steel to suppress external γ-rays. The main detector is covered by an outer veto system (not used in this analysis).

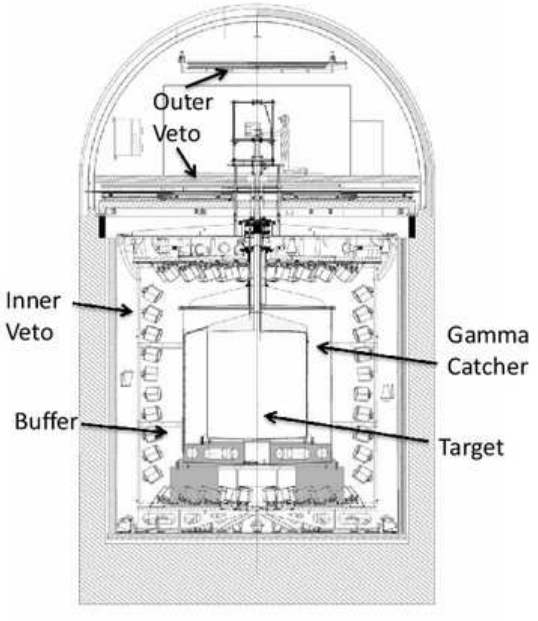

FIG. 1. A cross-sectional view of the Double Chooz detector system.

The detector is triggered by custom energy sum trigger electronics [37]. The ID PMTs are separated into two groups of 195 PMTs uniformly distributed throughout the volume and the PMT signals in each group are summed. The signals of the IV PMTs are also summed. The trigger is satisfied if any of the three sums is above a set energy threshold. The detector readout is based on 500 MHz flash-ADC electronics [38, 39] with customized firmware and a deadtime-free acquisition system. Upon each trigger, a 256 ns interval of the waveforms of both ID and IV signals is recorded. The low trigger rate (120 Hz) allowed the ID readout threshold to be set at 350 keV, well below the 1.02 MeV minimum energy of an IBD positron signal, greatly reducing the threshold systematics.

The experiment is calibrated using light sources, radioactive point sources, cosmic rays, and natural radioactivity. A multi-wavelength LED–fiber light injection system (LI) is used to inject fast light pulses illuminating the PMTs from fixed positions. Radio-isotopes ^{137}Cs, ^{68}Ge, ^{60}Co, and ^{252}Cf, sealed in miniature capsules, are periodically deployed in the target and the gamma catcher. Deployments in the target are carried out along the vertical axis of symmetry using a motorized pulley-and-weight system, operated from a glovebox. In the gamma catcher, the source is attached to a motor-driven wire and guided through a rigid hermetic loop, which traverses interior regions of the gamma catcher and passes along boundaries with the target and the buffer. The detector was regularly monitored using spallation neutron captures on H and Gd, residual natural radioactivity, and daily LI runs. The energy response was found to be stable to within 1% over time.

The signature of IBD events is a delayed coincidence between a prompt energy deposition, E_{prompt}, by the positron, and a later energy deposition, E_{delay}, due to the neutron capture on H or Gd within Δt_{e^+n} . In this analysis, a $\bar{\nu}_e$ event is defined by a capture on Gd, thus

constraining the fiducial volume to the target vessel without specific position cuts. The basis of the analysis is to compare the number of detected events, as well as their energy distribution, to a prediction based on the reactor data. We thus need an unbiased knowledge of the energy scale and need to identify the IBD events from background processes.

Energy measurements are based on the total charge, Q_{tot}, collected by the PMTs and corrected for gain variation. The energy is reconstructed by scaling Q_{tot} by a constant, adjusted so that the reconstructed energy of the gamma emitted following neutron capture on Hydrogen is 2.22 MeV at the center of the target. The energy scale corresponds to approximately 200 pe per MeV. Our Monte Carlo (MC), based on GEANT4 [40], is used to model the detector response and to calculate its acceptance. The MC includes parameters for quenching[41], absorption, re–emission, refraction, etc. which were determined from laboratory bench measurements of the detector liquids. Comparisons between actual and simulated calibration data in the target and gamma catcher were used to develop a parametric function, dependent on energy and vertex position, to correct the simulation, as well as to assess the uncertainties in the energy reconstruction. The correction ranges from -3% to +5 % for 0.7-10.0 MeV and, throughout the volume of the target, the range of the correction is 0% to -6%.

The following criteria are applied to distinguish $\bar{\nu}_e$ events from the background due to random coincidences and correlated coincidences induced by cosmic muons. Triggers within a 1000 μs window following a cosmic ray muon crossing the IV or the ID (46 s^{-1}) are rejected in order to reduce spallation neutron and cosmogenic backgrounds. This requirement is followed by five selections: 1) a cut rejecting events caused by some sporadically glowing PMT bases, resulting in light localized to a few PMTs and spread out in time: Q_{max}/Q_{tot} <0.09 (0.06) for the prompt (delayed) energy and rms(t_{start})< 40 ns, where Q_{max} is the maximum charge recorded by a single PMT and rms(t_{start}) is the standard deviation of the times of the first pulse on each PMT; 2) 0.7 MeV<E_{prompt}<12.2 MeV; 3) 6.0 MeV <E_{delay}<12.0 MeV; 4) 2 μs < Δt_{e^+n} < 100 μs, where the lower cut is applied to eliminate correlated noise and the upper cut is determined by the $\sim$ 30 μs capture time on Gd; 5) a multiplicity cut to reject correlated backgrounds defined as no additional valid trigger from 100 μs preceding the prompt candidate to 400 μs after it.

Applying selections (1-5) yields 4121 candidates or 42.6 $\pm$0.7 events/day for an analysis live time of 96.8 days. Their spatial distribution is uniform within the target vessel.

Some uncorrelated and correlated (fast neutrons, stopping muons and ^{9}Li and ^{8}He β-n emitters) background events survive these cuts and their contribution have been estimated. Uncorrelated coincidences are dominated by the random association of a prompt energy deposition due to radioactivity (7.6 s^{-1}) and a delayed neutron capture ($\simeq$20/hour). This background is measured by applying selection cuts (1-5) but modifying selection (4) such that the 2-100 μs time window is shifted by 1000 μs relative to the prompt trigger. To improve the precision of this random background measurement, 198 such windows, each shifted from the previous one by 500 μs, were used, leading to 0.33 ± 0.03 events per day.

Fast neutrons induced by muons traversing the surrounding rock can interact in the target producing a recoil proton and then be captured, thus simulating an IBD event. We estimate the total rate to be 0.83 $\pm$ 0.38 events per day (including a contribution from stopping muons) by applying cuts (1-5), but modifying selection (2) such that 12.2 MeV < E_{prompt}<30 MeV, and then extrapolating to the signal region, assuming a flat energy spectrum. We account for an uncertainty in this extrapolation, and for the contribution of stopping muons, by including a shape error ranging up to $\pm$ 70% of the flat extrapolation at lower energies.

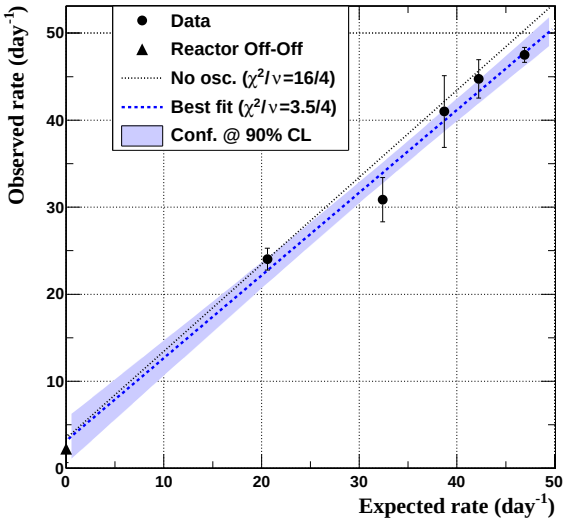

FIG. 2. Daily number of $\bar{\nu}_e$ candidates as a function of the expected number of $\bar{\nu}_e$. The dashed line is a fit to the data, the band is the 90% CL of this fit. The dotted line is the expectation in the no-oscillation scenario. The triangle indicates the one day measurement with both reactors off.

The ^{9}Li β-n emitters are produced preferentially by energetic muons. They were studied by searching for a triple delayed coincidence between a muon depositing > 600 MeV in the detector and a $\bar{\nu}_e$ -like pair of events, where the delay between the muon and prompt event is dictated by the long, 178 ms, halflife of ^{9}Li, which precludes vetoing on all muons. Fitting the resulting time distribution with a flat component and an exponential with the ^{9}Li lifetime results in an estimated rate of 2.3 ± 1.2 events per day. This rate is assumed to have the energy spectrum expected from the ^{9}Li decay branches. An uncertainty in the shape of up to 20% is introduced to

account for uncertainties in some decay branches. ^{8}He is not considered since it is less abundantly produced [42].

The overall background envelope is independently verified by analyzing 22.5 hours of both-reactors-off data (< 0.3 residual $\bar{\nu}_e$ events). Two $\bar{\nu}_e$ candidates with prompt energies of 4.8 MeV and 9.8 MeV pass cuts (1-5). They could be associated spatially within 30 cm, and in time within 220 ms, with the closest energetic muon, and are thus likely to be associated with ^{9}Li.

The total background rate is estimated to be 3.45 ± 1.26 d^{-1} and is summarized in Table I.

Background	Rate (D^{-1})	Syst. Uncertainty (% of signal)
Accidental	0.33 ± 0.03	< 0.1
Fast neutron	0.83 ± 0.38	0.9
^{9}Li	2.3 ± 1.2	2.8

TABLE I. The breakdown of the estimated background rate. Additional shape uncertainties are described in the text.

Several corrections and efficiencies were evaluated using the MC and their uncertainties included in the final result. The energy response introduces a 1.7% systematic uncertainty determined from fits to calibration data. The number of free protons inside the target, 6.747×10^{29} based on a weight measurement of the target scintillator, has an uncertainty of 0.3%, originating from the knowledge of the hydrogen ratio in the scintillator. A dedicated simulation including molecular bond effects [43] indicates that the number of IBD events occurring in the gamma catcher with the neutron captured in the target (spill in) exceeds the number of events occurring in the target with the neutron escaping to the gamma catcher (spill out) by $1.4\% \pm 0.4\%$, 0.8% lower than our standard MC prediction which was therefore reduced accordingly. Above the 700 keV analysis threshold, the trigger efficiency is $100.0^{+0}_{-0.4}\%$, assessed with a low threshold down-scaled trigger. Calibration data taken with the ^{252}Cf source were used to check the MC for any biases in the neutron selection criteria and estimate their contributions to the systematic uncertainty. The fraction of neutron captures on Gd is evaluated to be $(86.0 \pm 0.5)\%$ near the center of the target, 2.0% lower than the simulation prediction which was therefore reduced accordingly with a relative systematic uncertainty of 0.6%. The simulation reproduces the 96.5% efficiency of the Δt_{e^+n} cut with an uncertainty of 0.5%. The fraction of neutron captures on Gd accepted by the 6.0 MeV cut, 94.5%, agrees with calibration with an uncertainty of 0.6%. The MC normalization was adjusted further for the muon veto (-4.5 %) and the multiplicity veto (-0.5 %) dead-times.

We modeled the $\bar{\nu}_e$ production in each reactor core and their interactions in the detector with a comprehensive propagation of uncertainties including all known correlations. The full covariance matrix of the emitted $\bar{\nu}_e$ spectra was computed as prescribed in [31]. The MURE reactor simulations provided the fission rate covariance matrix. The resulting uncertainties on the ^{235}U, ^{239}Pu, ^{238}U and ^{241}Pu fission rates are ±3.3%, ±4%, ±6.5% and ±11% respectively.

Detector		Reactor	
Energy response	1.7%	Bugey4 measurement	1.4%
E_{delay} Containment	0.6%	Fuel Composition	0.9%
Gd Fraction	0.6%	Thermal Power	0.5%
Δt_{e^+n}	0.5%	Reference Spectra	0.5%
Spill in/out	0.4%	Energy per Fission	0.2%
Trigger Efficiency	0.4%	IBD Cross Section	0.2%
Target H	0.3%	Baseline	0.2%
Total	2.1 %	Total	1.8%

TABLE II. Contributions (in %) of the detector and reactor errors to the overall systematic uncertainties on the absolute normalization factor.

To avoid being affected by possible very short baseline $\bar{\nu}_e$ oscillations [4, 44, 45] we adopt the reactor $\bar{\nu}_e$ spectrum of [27, 31], but we normalize the cross section per fission to the Bugey4 measurement[18] accounting for differences in core inventories ($0.9 \pm 1.3\%$ correction), and including a 1.4% uncertainty in the Bugey4 measurement. The IBD differential cross section is taken from[11], but using 881.5 ± 1.5 s [1] as the neutron lifetime. The expected number of $\bar{\nu}_e$ candidates is 4344±165, including background.

These systematic uncertainties are summarized in Table II.

The power of the two reactors varied during our data taking period. The measured daily rate of IBD candidates as a function of the expected rate for different reactor powers assuming no oscillations is shown in Figure 2. The extrapolation to zero reactor power of the best fit to the data yields 3.2±1.2 events per day in excellent agreement with our estimate and the both-reactors-off data.

The ratio of observed to expected events is $R_{DC} = 0.944 \pm 0.016(\text{stat.}) \pm 0.040(\text{syst.})$, corresponding to $\sin^2 2\theta_{13} = 0.104 \pm 0.030(\text{stat}) \pm 0.076(\text{syst})$.

The analysis is improved by comparing the positron spectrum in 18 variably sized energy bins between 0.7 and 12.2 MeV to a simulation of the expected number of $\bar{\nu}_e$ events . The analysis is performed with a standard χ^2 estimator, using a set of four covariance matrices to include uncertainties in the antineutrino signal, detector response, signal and background statistics, and background spectral shape. Very few positrons are expected above 8 MeV. Thus the region 8–12.2 MeV reduces the uncertainties in the correlated backgrounds with some additional contribution to the statistical uncertainty.

The best fit results in $\sin^2 2\theta_{13} = 0.086 \pm 0.041$ (stat) ± 0.030 (syst) with a χ^2/DOF of 23.7/17. Using a frequentist approach [46] we find an allowed region of $0.015 < \sin^2 2\theta_{13} < 0.16$ at 90% CL, and exclude the no oscillation hypothesis at the 94.6% C.L..

We determine our best estimate of the $\bar{\nu}_e$ and background rates with a pulls-based approach[47]. From the best fit we obtain a contribution from ^{9}Li which is re-

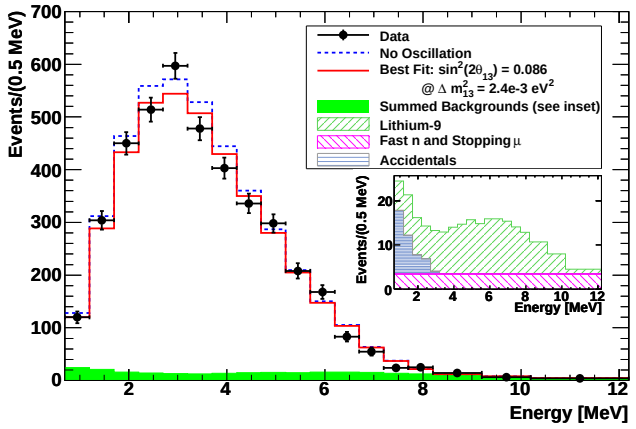

FIG. 3. Expected visible energy spectra, including neutrinos and backgrounds, for the no-oscillation case and for the best fit value of $\sin^2 2\theta_{13}$, superimposed on the measured positron spectrum. Inset: stacked histogram of backgrounds.

duced by ∼19%, and with an uncertainty which has decreased from 52% to 26%. The fast neutrons value is decreased by 5% with almost unchanged uncertainty. Figure 3 shows the measured positron spectrum superimposed on the expected spectra for the no-oscillation hypothesis and for the best fit (including a priori backgrounds).

The combination of our result with the T2K [12] and MINOS [13] measurements leads to $0.003 < \sin^2 2\theta_{13} < 0.219$ at the 3σ level.

The predicted experimental cross section per fission is $\sigma_f^{pred} = (5.703 \pm 0.108)\,10^{-43}$ cm^2/fission based on the Bugey4 anchoring measurement, corrected to match our fractions of fissions per isotope ^{235}U=48.8%, ^{239}Pu=35.9%, ^{241}Pu=6.7%, and ^{238}U=8.7%. Not including the Bugey4 measurement, $\sigma_f^{pred} = (6.209 \pm 0.170)\,10^{-43}$ cm^2/fission based on the improved reference spectra [27, 31]. This can be compared to our measured crossection per fission at the far detector $\sigma_f^{pred} = (5.383 \pm 0.210)\,10^{-43}$ cm^2/fission.

In summary, Double Chooz has used 101 days of reactor data combined with a 10 m^3 detector located 1050 m away, to search for $\bar{\nu}_e$ disappearance. A total of 4121 events were observed where 4344 ± 165 were expected in the no-oscillation case, with a signal to background ratio in the prompt energy window of ≈ 11:1. Interpreted in the context of neutrino oscillations, this deficit leads to a value $\sin^2 2\theta_{13} = 0.086 \pm 0.041$ (stat) ± 0.030 (syst), based on an analysis using rate and energy spectrum information. The no-oscillation hypothesis is ruled out at the 94.6 % C.L.. Double Chooz continues to run, focusing on the reduction of the statistical and background systematic uncertainties. A near detector will soon be on-line allowing reduced reactor and detector induced systematic uncertainties leading to an estimated 1 σ precision on $\sin^2 2\theta_{13}$ of ∼ 0.02.

We thank all the technical and administrative people who helped build the experiment. We thank, for their participation, the French electricity company EDF, the European fund FEDER, the Région de Champagne Ardenne, the Département des Ardennes and the Communauté des Communes Rives de Meuse. We acknowledge the support of CEA and CNRS/IN2P3 in France, MEXT and JSPS of Japan, the Department of Energy and the National Science Foundation of the United States, the Ministerio de Ciencia e Innovación (MICINN) of Spain, the Max Planck Gesellschaft and the Deutsche Forschungsgemeinschaft DFG (SBH WI 2152), the Transregional Collaborative Research Center TR27, the Excellence Cluster "Origin and Structure of the Universe" and the Maier-Leibnitz-Laboratorium Garching, the Russian Academy of Science, the Kurchatov Institute and RFBR (the Russian Foundation for Basic Research), the Brazilian Ministry of Science, Technology and Innovation (MCTI), the Financiadora de Estudos e Projetos (FINEP), the Conselho Nacional de Desenvolvimento Científico e Tecnológico (CNPq), the São Paulo Research Foundation (FAPESP) and the Brazilian Network for High Energy Physics (RENAFAE) in Brazil.

[1] K. Nakamura et al., J. Phys. G **37**, 075021 (2010).
[2] B. Pontecorvo, JETP **34**, 172 (1958).
[3] Z. Maki, M.Nakagawa, and S. Sakata, Prog. Theor. Phys. **28**, 870 (1962).
[4] M. Appolonio et al., Phys. Lett. **B466**, 415 (1999).
[5] F. Boehm et al., Phys.Rev. Lett. **84**, 3764 (2000).
[6] H. Minakata et al., Phys. Rev. D **68**, 033017 (2003).
[7] H. Minakata et al., Phys. Rev. D **70**, 059901 (2003).
[8] P. Adamson et al. (MINOS Collaboration), Phys.Rev.Lett. **106**, 181801 (2011).
[9] X. Guo et al. (Daya Bay Collaboration) (2006), arXiv:hep-ex/0701029.
[10] J. K. Ahn et al. (RENO Collaboration) (2010), arXiv:hep-ex/1003.1391.
[11] P. Vogel and J. F. Beacom, Phys. Rev. D **60**, 053003 (1999).
[12] K. Abe et al. (T2K Collaboration), Phys.Rev.Lett. **107**, 041801 (2011), 1106.2822.
[13] P. Adamson et al., Phys. Rev. Lett. **107**, 181802 (2011), hep-ex/1108.0015v1.
[14] T. Schwetz et al. (2011), hep-ph/1108.1376v1.
[15] G. L. Fogli et al. (2011), hep-ph/1106.6028v2.
[16] F. Ardellier et al. (Double Chooz Collaboration) (2006), hep-ex/0606025v4.
[17] G. Mention, Ph.D. thesis (2005), URL `http://tel.archives-ouvertes.fr/tel-00010528/fr/`.
[18] Y. Declais et al., Phys. Lett. **B338**, 383 (1994).
[19] S. F. E. Tournu et al., EPRI 2001.1001470, Palo Alto, CA. (2001).
[20] Standard AFNOR XP X 07-020, Palo Alto, CA. (1996).

[21] O. Meplan, Tech. Rep. LPSC 0912 and IPNO-09-01 (2009).

[22] MURE, *Mcnp utility for reactor evolution: couples monte-carlo transport with fuel burnup calculations* (2009), URL http://www.nea.fr/tools/abstract/detail/nea-1845.

[23] R. R. G. Marleau and A. Hebert, Tech. Rep. IGE-157 (1994).

[24] C. Jones et al. (2011), nucl-ex/1109.5379v1.

[25] V. Kopeikin et al., *Reactor as a source of antineutrinos: Thermal fission energy* (2004), hep-ph/0410100v1.

[26] *Jeff and eff projects*, URL http://www.oecd-nea.org/dbdata/jeff/.

[27] P. Huber, Phys. Rev. C **84**, 024617 (2011).

[28] W. G. K. Schreckenbach, G. Colvin and F. von Feilitzsch, Phys. Lett. B **160** (1985).

[29] A. F. von Feilitzsch and K. Schreckenbach, Phys. Lett. B **118** (1982).

[30] A. A. Hahn et al., Phys. Lett. B **218** (1989).

[31] T. Mueller et al., Phys. Rev. C **83**, 054615 (2011).

[32] C. Aberle et al., *Large scale gadolinium-beta-diketonate based organic liquid scintillator production for antineutrino detection*, In preparation.

[33] C. Aberle et al., Chem. Phys. Lett. **516**, 257 (2011).

[34] T. Matsubara et al., Nucl.Instrum.Meth. in Physics Research **A661**, 16 (2011), 1104.0786[phys.ins-det].

[35] C. Bauer et al., JINST **6**, P06008 (2011), 1104.0758.

[36] E. Calvo et al., Nucl.Instrum.Meth. in Physics Research **A621**, 222 (2010), 0905.3246[phys.ins-det].

[37] C. Kuhnt, Master's thesis (2010), URL http://www.physik.rwth-aachen.de/fileadmin/user_upload/www_

[38] A. Cabrera et al., Nucl.Instrum.Meth. in Physics Research **A617**, 473 (2010).

[39] T. Akiri, Ph.D. thesis (2010), URL http://tel.archives-ouvertes.fr/tel-00580175/fr/.

[40] S. Agostinelli et al., Nucl.Instrum.Meth. in Physics Research **A506**, 250 (2003).

[41] C. Aberle et al., JINST **6**, P11006 (2011).

[42] S. Abe et al., Phys. Rev. C **81**, 025807 (2010).

[43] J. P. Both et al., Tech. Rep. CEA-REPORT: CEA-R-6044, DTI, CEA/Saclay, France (2003).

[44] G. Mention et al., Phys. Rev. D **83**, 073006 (2011).

[45] C. Giunti and M. Laveder (2011), hep-ph/1111.5211v2.

[46] G. J. Feldman and R. D. Cousins, Phys. Rev. D **57**, 3873 (1998).

[47] D. Stump et al., Phys. Rev. D **65**, 014012 (Appendix B) (2001).